iScience, Volume *25*

Supplemental information

Immune translational control by CPEB4 regulates intestinal inflammation resolution and colorectal cancer development

Annarita Sibilio, Clara Suñer, Marcos Fernández-Alfara, Judit Martín, Antonio Berenguer, Alexandre Calon, Veronica Chanes, Alba Millanes-Romero, Gonzalo Fernández-Miranda, Eduard Batlle, Mercedes Fernández, and Raúl Méndez

Figure S1. Characterization of gut and systemic CPEB4 depletion, related to Figure1

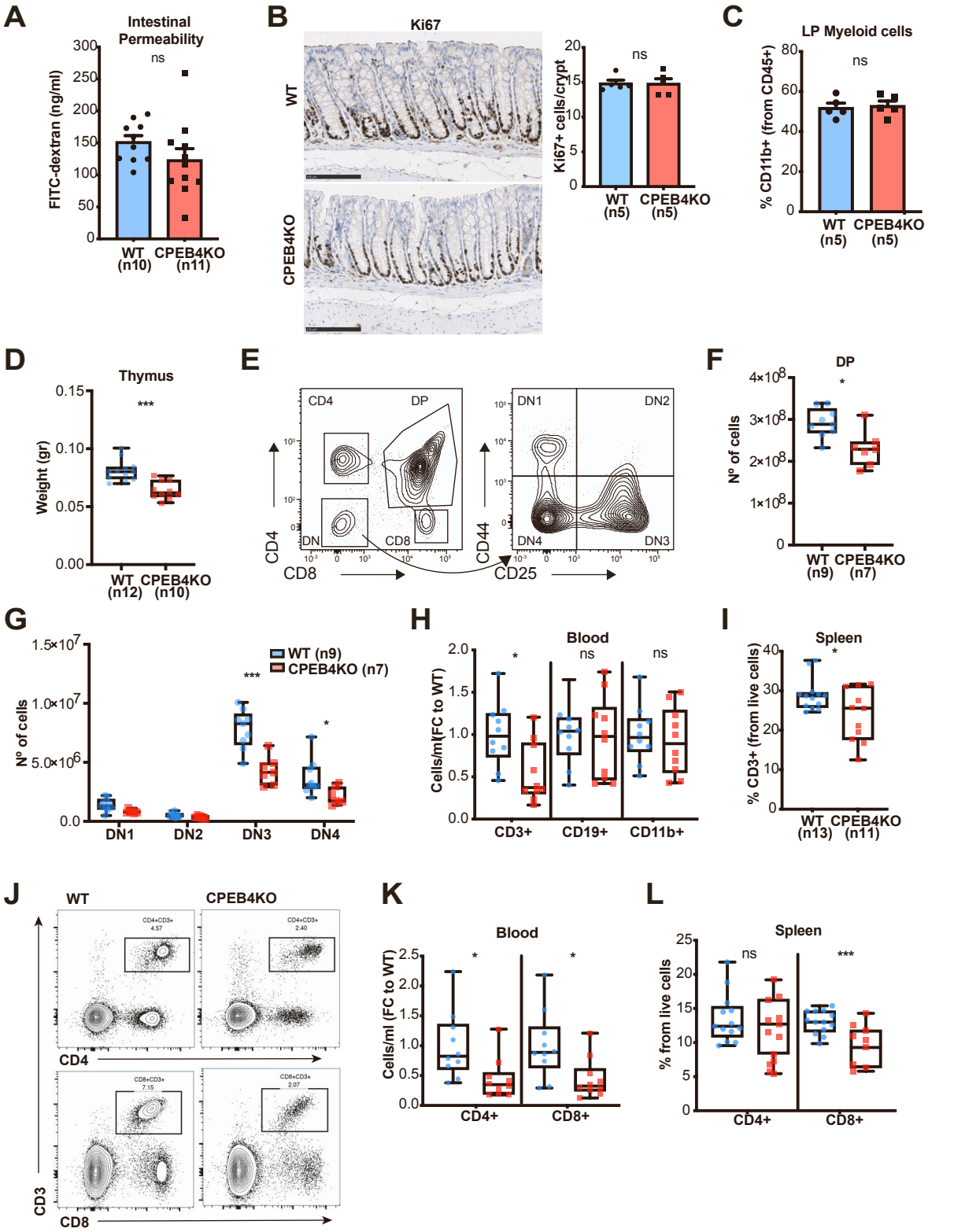

Figure S2. Characterization of CPEB4-depleted mice during DSS-colitis resolution, related to Figure 2

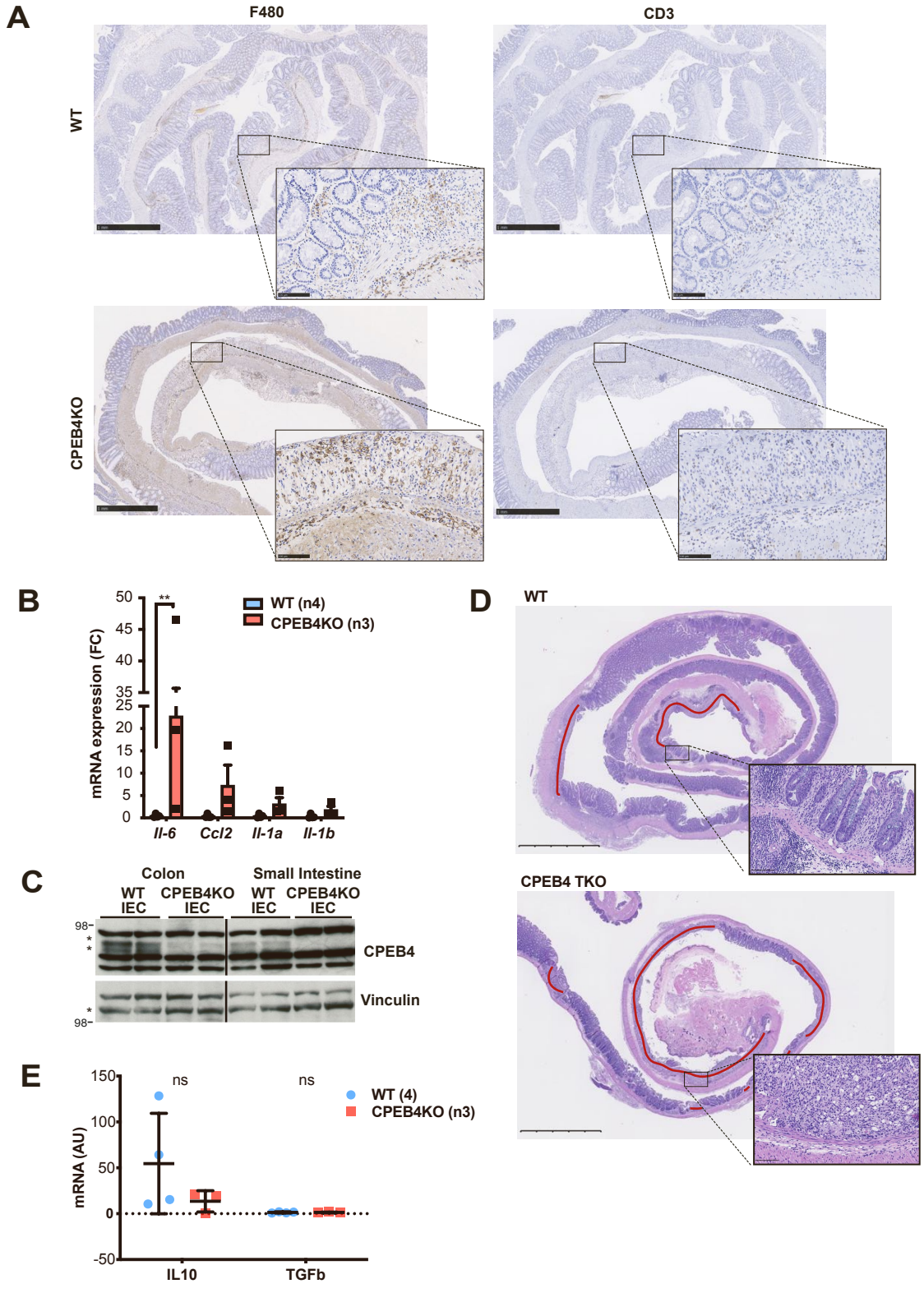

Figure S3. Characterizaion of IL-22 signaling in WT and CPEB4KO mice, related to Figure 4

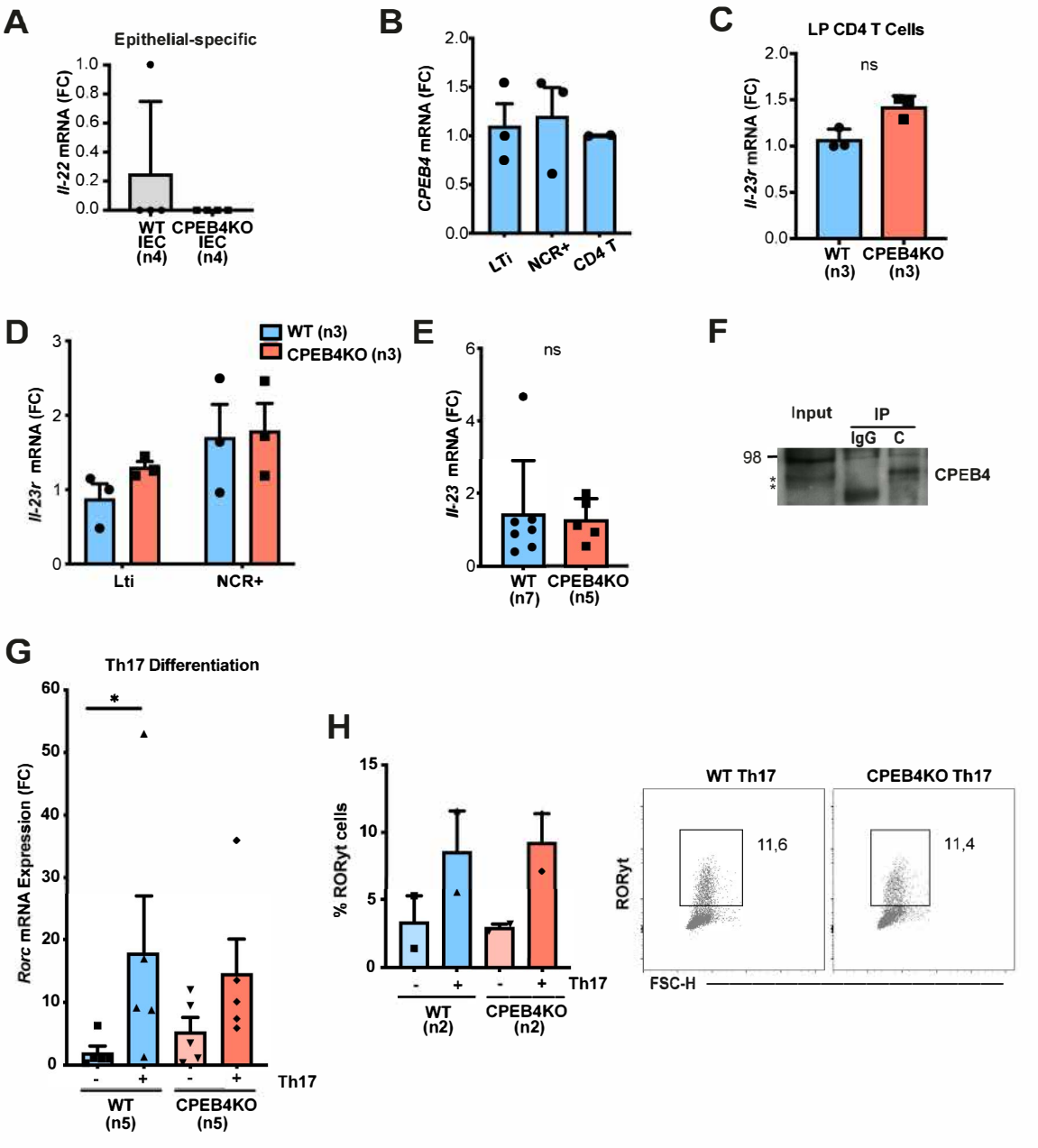

Figure S4. Characterization of WT and CPEB4KO AOM/DSS tumors, related to Figure 5

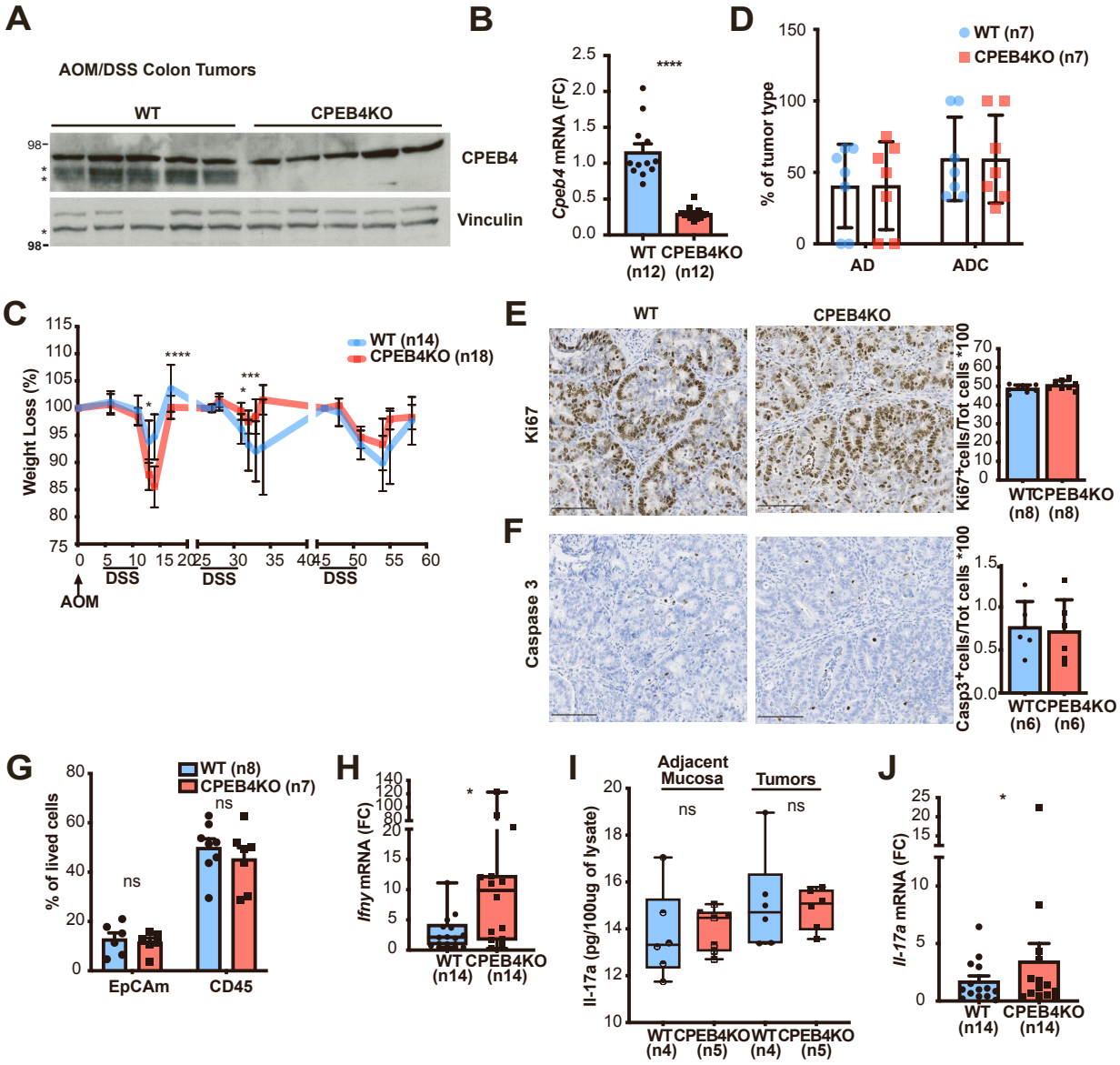

Figure S5. CPEB4 accumulates in the immune cell population of AOM/DSS tumors, related to Figure 6

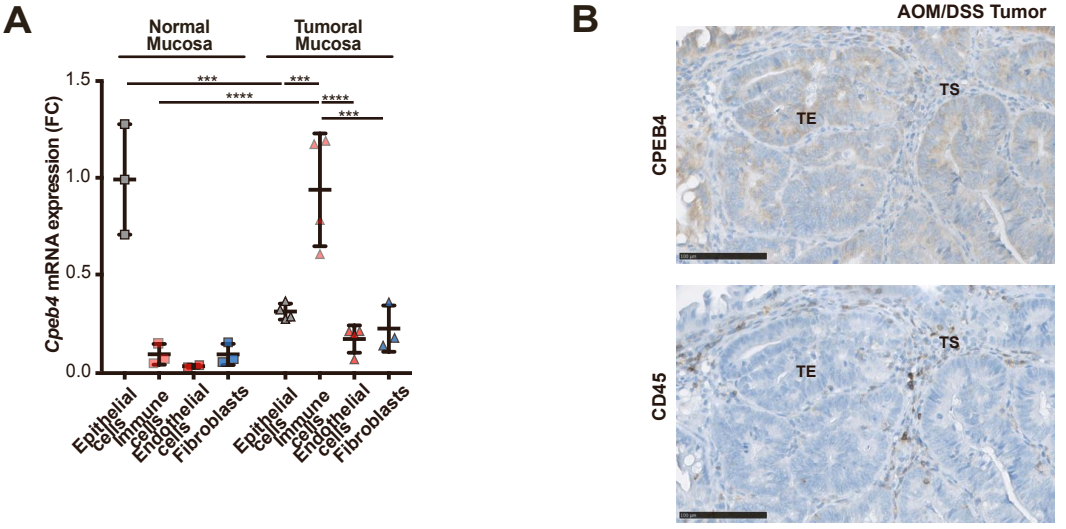

SUPPLEMENTAL INFORMATION

SUPPLEMENTAL FIGURE LEGENDS

Figure S1. Characterization of gut and systemic CPEB4 depletion, related to Figure 1.

(A) Intestinal permeability in WT (n=10) and CPEB4KO (n=11) mice was measured by determining the concentration of FITC-dextran in blood serum. Mean ± SEM, *P*=0,0986. (*B*) Representative stainings and relative quantification of Ki67 and IHC from WT and CPEB4KO untreated colons. *(C)* WT and CPEB4KO lamina propria (LP) myeloid cells ($CD11b^+$) were analysed from $CD45^+$ cells by flow cytometry analysis. *(D)* Thymus weight of WT (n=12) and CPEB4KO (n=10) mice. Mean ± SEM. ***P=0.0002. *(E)* Representative plots of thymus populations analysis by FACS. *(F,G)* Number of double positive (DP) *(F)* and double negative (DN) *(G)* populations of WT (n=9) and CPEB4KO (n=7) thymus. Mean ± SEM. (F) *P=0.0115 (Mann-Whitney); (G)***P<0.0001, *P=0.0111. *(H)* Blood immune phenotyping of WT and CPEB4KO mice (n=10/genotype) by FACS analysis. The data are shown as FC to WT of cells/ml. CD3, *P=0.0116; (unpaired *t*-test). *(I)* Spleen samples from unchallenged WT (n=13) and CPEB4KO (n=11) mice were analyzed by FACS for CD3+. Data are shown as percentages from live cells (mean ± SEM). *P=0.0267. *(J)* Representative plots of blood analysis by FACS. *(K)* CD4+ and CD8+ cells/ml and representative plots of cytometry analysis of WT and CPEB4KO blood samples. The stainings are indicated. CD4, *P=0.0151; CD8, *P=0.0166 (Unpaired *t*-test). *(L),* Percentage of CD4+ and CD8+ from spleen of WT and CPEB4KO mice. ***P=0.0007 (Unpaired *t*-test). Data are pooled of two (A) and three (C,D,F,G,H,I,K,L) biologically independent experiments.

Figure S2: Characterization of CPEB4-depleted mice during DSS-colitis resolution, related to Figure 2.

(A) Representative stainings of F480 and CD3 IHC from WT and CPEB4KO DSS-treated colons at day 10. Scale bars, 1 mm; larger magnification 100µm. *(B*) Relative mRNA expression levels of *Il-6, Ccl2*, *Il-1a* and *Il-1b* in colon of DSS-treated WT and CPEB4KO mice at day 10 were determined by qPCR. Expression levels were measured as fold change (FC) of treated WT mice for each gene. Data are mean ± SEM; **P=0.0041 (two-way ANOVA test, multiple comparisons). *(C)* CPEB4 protein expression in colon and small intestine lysates after 5 days of tamoxifen treatment in WT and CPEB4 intestine-specific KO mice. Vinculin was used as loading control. * Shows specific bands. (*D*) Representative H&E-stained colon sections from DSS-treated WT and CPEB4 TKO mice, analyzed at day 11. The regenerating region is highlighted with a red line. Scale bars, 2.5 mm. Larger magnification 100µm.

Figure S3: Characterization of IL-22 signaling in WT and CPEB4KO mice, related to Figure 4.

(*A) Il-22* mRNA expression in colon extracts of epithelial specific WT and CPEB4KO mice (n=4/genotype). Data are normalized by *Gapdh*. (*B*) *Cpeb4* mRNA expression in LTi and NCR+ (ILC3) and CD4+ T cells from lamina propria of WT mice. (*C*) *Il-23r* mRNA expression in CD4 T cells (n=3) and (*D*) Lti and NCR^+ ILC3 cells (n=3) from lamina propria (means ± SEM). (*E*) *Il-23* mRNA expression in colon extracts of WT (n=7) and CPEB4KO (n=5) mice. (*F*) Representative CPEB4 western blot of RNA immunoprecipitation experiment in Th17 differentiated CD4 cells. (*G,H*) *Rorc* mRNA and RORyt protein expression in WT and CPEB4KO CD4 T cells stimulated or not to induce Th17 differentiation. *P=0,0159 (Mann-Whitney test between WT and WT Th17).

Figure S4: Characterization of WT and CPEB4KO AOM/DSS tumors, related to Figure 5.

(*A,B*) CPEB4 protein and mRNA expression in AOM/DSS colon tumors from WT and CPEB4KO mice. * Shows specific bands; ***P=0.0002 (Mann-Whitney test). *(C)* Percentage

of body weight loss after AOM/DSS treatment in WT (n=14) and CPEB4KO (n=18) mice. **P*=0.0136, *****P*<0.0001, **P*=0.0182, ****P*=0.0002 (two-way ANOVA test, multiple comparisons). *(D)* Percentage of tumor types, polypoid and flat adenomas (AD) and adenocarcinomas (ADC). The presence of one type of tumor was set as 100%. (*E,F*) Representative images and related quantifications of colon tumors immunostained for Ki67 (WT, n=8; CPEB4KO, n=8) and Caspase 3 (WT, n=6; CPEB4KO, n=6) at end point. Scale bars, 100 µm. *(G)* $Epcam^+$ and $CD45^+$ populations of colon tumors from WT and CPEB4KO mice were gated from lived cells. *(H) Ifnγ* mRNA levels, relative to *Gapdh*, in total colon tumor extracts from WT and CPEB4KO mice (n=14/genotype). **P*=0.0163 (Mann-Whitney test). (*I*) ELISA of il-17a in adjacent mucosa and AOM-DSS tumors of WT (n=6) and CPEB4KO (n=6) mice. *(J)* Relative *il-17a* mRNA levels in WT (n=14) and CPEB4KO (n=14) tumors analysed by RT-qPCR. **P*=0,5 (unpaired *t*-test).

Figure S5. CPEB4 accumulates in the immune cell population of AOM/DSS tumors, related to Figure 6. (*A*) Relative mRNA expression levels (fold change, FC) of *Cpeb4* in normal and tumoral mucosa of untreated and AOM/DSS-treated WT mice, respectively, were determined by RT-qPCR. Data are means ± SD. ****P*=<0.005; *****P*<0.0001 (two-way ANOVA test, multiple comparisons). (*B*) Representative stainings of CPEB4 and CD45 in AOM/DSS-induced tumors from WT mice. Scale bars, 100 µm.

Table S1_Primers used for Real Time qPCR_related to STAR Methods		
Gene	Forward	Reverse
mCpeb4	CCAGAATGGGGAGAGAGTGG	CGGAAACTAGCTGTGATCTCATCT
mIl-17a	GCTCCAGAAGGCCCTCAGA	CTTTCCCTCCGCATTGACA
mIl-17f	TCCCCTGGAGGATAACACTG	GGGGTCTCGAGTGATGTTGT
mIl-1a	GAGAGCCGGGTGACAGTATC	TGACAAACTTCTGCCTGACG
mIl-1b	GGGCCTCAAAGGAAAGAATC	TACCAGTTGGGGAACTCTGC
mIl-6	AGTTGCCTTCTTGGGACTGA	CAGAATTGCCATTGCACAAC
mIl-10	GGTTGCCAAGCCTTATCGGA	GAGAAATCGATGACAGCGCC
mIl-22	TCCGAGGAGTCAGTGCTAAA	AGAACGTCTTCCAGGGTGAA
mTNFα	CTATGGCCCAGACCCTCACACTC	GCTGGCACCACTAGTTGGTTGTCTT
mIFNγ	AACTGGCAAAAGGATGGTGAC	TTGCTGATGGCCTGATTGTC
mCcl2	TTTTGTCACCAAGCTCAAGAGA	ATTAAGGCATCACAGTCCGAGT
mIl-23R	AGAGACACTGATTTGTGGGAAAG	GTTCCAGGTGCATGTCATGTT
mSaa1/2	AGTGGCAAAGACCCCAATTA	GGCAGTCCAGGAGGTCTGTA
mAngiogenin 4	TTGGCTTGGCATCATAGT	CCAGCTTTGGAATCACTG
mIl-22ra2	TATTTTGCACTGGCAAGCAG	CCCATTGGCTCTGTCCATAC
mGapdh	CTTCACCACCATGGAGGAGGC	GGCATGGACTGTGGTCATGAG
mHPRT	TATGGCGACCCGCAGCCCT	CATCTCGAGCAAGACGTTCAG
mTBP	AGAACAATCCAGACTAGCAGCA	GGGAACTTCACATCACAGCTC

Table S2_ GEO Datasets used_related to STAR Methods
Colorectal cancer datasets:
GSE33113
GSE14333
GSE39582
GSE38832
GSE44076
GSE39395
GSE39396
GSE35602
Adult inflammatory bowel disease datasets:
GSE13367
GSE59071
GSE9452
GSE16879
Pediatric inflammatory bowel disease dataset:
GSE10616